Amrita Sinha[1*], D. N. Vishwakarma[2],

J. Electrical Systems 9-1 (2013): 125-136

Regular paper

Journal of Electrical Systems

Pattern Classification based Intelligent Numerical Protection of Salient-pole Synchronous Generator using Neural Networks

This paper presents the application of neural networks for the non-differential protection of salient-pole synchronous generator against internal faults in any winding of the stator. The direct phase quantities and modified winding function approach has been used to simulate different types of internal and external faults using electrical parameters of generators installed by utilities. The cases of all the possible types of internal faults in the stator winding have been taken into consideration in designing the protection scheme. Multi-layer Feed-forward Neural Network (MFNN) and Radial Basis Function Neural Network (RBFNN) have been trained and tested for detection, identification and classification of the internal faults based on pattern classification. The simulated fault currents in the phases as well as their parallel paths at the terminal end have been used for training and testing of both the proposed neural networks. Both the networks are able to identify the fault signal correctly but the MFNN is more reliable, more accurate and faster than RBFNN in detection and classification of the fault.

Keywords: Synchronous generator protection; Artificial Neural Network; Multi-Layer Feed-Forward Network; Radial Basis Function Neural Network; Pattern classification.

1. Introduction

Hydro-electric power stations which are integral parts of the modern power system use large salient pole synchronous generators due to low speed of the prime mover. These generators usually have wave-connected parallel stator windings in order to enhance their current ratings. The knowledge about the internal faults in the stator windings of these machines is very essential as the large fault currents may cause severe damage to the windings and possibly to the mechanical parts of the machine. In order to design an appropriate intelligent numerical protection scheme for synchronous generators to protect against the internal faults, it is essential to have complete knowledge about the fault data. However, it is impractical and very difficult to get actual fault data of synchronous generators. Therefore, simulation of various internal fault conditions of synchronous generator i.e. turn-to-turn, turn-to-frame etc. has been done which is more versatile and cost effective.

The field winding current has been used to detect fault in the armature winding using online digital computer technique in [1]. For discrimination of internal and external fault the direction of the negative sequence power flow at the machine terminals has been used in [2]. Based on positive and negative sequence calculation, a generalized digital technique has been developed for detecting open circuit and short circuit in the stator windings of the synchronous generator. A neural network based digital differential relay has been implemented for fault detection and fault classification using separate modules in [3]. The presence of fundamental and/or second harmonic component in the field current has been used for differentiating the three generator states (normal, internal fault and external fault). To detect the generator winding fault, classify the type of fault, and also identify the faulted phases, different fault diagnosis schemes based on artificial neural network have been

[*] Corresponding author: Amrita Sinha, Department of Electrical Engg., National Institute of Technology, Patna-800005, E-mail: amrita_bhu@yahoo.co.in

[2] Department of Electrical Engineering, Institute of Technology, Banaras Hindu university, Varanasi-221005

presented in [4]. For discrimination between the three operating states of the synchronous generator, a neuro-fuzzy based scheme has been proposed in [5], which operates only in the case of internal faults in the stator winding uses separate modules for detection and classification.

An efficient differential relay for classification of faults in power transformer has been demonstrated based on RBFNN in [6, 7]. Using radial basis function neural networks, many methodologies have been presented for transmission line fault detection, classification and its location [8, 9].

For designing the protection schemes in [3, 5], the internal fault simulation approach have assumed that the windings are concentrated or magneto-motive force in the air gap is sinusoidally distributed. The simulation of internal fault for synchronous generator in [4], has been done in EMTP environment.

This paper presents an intelligent numerical protection scheme for salient-pole synchronous generators based on Multi Layer Feed Forward Neural Networks (MFNN) and Radial Basis Function Neural Networks (RBFNN), where the protection philosophy is viewed as a pattern classification problem. The synchronous machine model based on direct phase quantities and Modified Winding Function Approach (MWFA) has been used for simulating internal and external faults under different conditions. The MWFA calculates the machine inductances using the turns function of the parallel paths directly derived from the stator winding arrangement. The MWFA requires the electrical parameters and the winding diagram of the synchronous generator for the calculation of self and mutual inductances therefore the simulation of faults can't be generalized. Various architectures of feed-forward neural networks has been trained and tested using simulated numerical fault data, and the most suitable architecture of ANN which will give the correct information regarding occurrence of the internal fault in the machine has been identified. Similarly, various networks has been trained and tested with different spread constants and the most suitable architecture of RBFNN has been identified. The proper tripping command can be issued to the circuit breaker to isolate the faulty generator, after receiving the signal of occurrence of the fault.

2. Inductance Calculation based on MWFA

The synchronous machine model based on direct phase quantities and Modified Winding Function Theory requires access to the stator winding arrangement for deriving the turns function. The fault simulation can be generalized for only the machines of the same make and size with identical stator winding arrangement. The MWFA has been used to simulate different types of internal and external faults using machine electrical parameters instead of the geometrical ones [10]. The inductances are derived directly from the original waveforms using turns function of the actual machine winding distribution; hence the space harmonics are taken into account. Other than the calculation of the self and mutual inductances of the individual parallel paths of the machine, the equations are similar to direct phase quantities mathematical model of synchronous generator.

The Modified Winding Function Theory as expressed in equation (1) & (2) and discussed by [11], is used in this paper to take into account the effect of the non-uniform air gap and non-sinusoidally distributed windings in case of internal faults in large synchronous generators.

$$L_{xy} = 2\pi\mu_0 rl\left\langle g^{-1}(\theta,\phi) n_x(\theta,\phi) n_y(\theta,\phi)\right\rangle - 2\pi\mu_0 rl\frac{\left\langle g^{-1}(\theta,\phi) n_x(\theta,\phi)\right\rangle\left\langle g^{-1}(\theta,\phi) n_y(\theta,\phi)\right\rangle}{\left\langle g^{-1}(\theta,\phi)\right\rangle} \qquad (1)$$

Where, μ_0 is the permeability of the free space,

r is the average radius of the air gap,

l is the axial stack length of the machine,

$g^{-1}(¨,¯)$ is the inverse air gap length,

and $n_x(¨,¯)$ and $n_y(¨,¯)$ are the turns function of the windings *x* and *y*, respectively.

Here, ¨ is the angle along the inner surface of the stator,

and θ is the angular position of the rotor with respect to the stator reference axis.

Operator $\langle f \rangle$ is defined as the mean value of function *f* over [*0,2π*] as follows:

$$\langle f \rangle = \frac{1}{2®} \int_0^{2®} f(¨)d¨ \tag{2}$$

For a 2*p* salient-pole synchronous machine analysis, the inverse air gap length is usually approximated as [12],

$$g^{-1}(¨,¯) = ~_0 - ~_2 \cos(2p - ¯) \tag{3}$$

Where, the minimum air-gap length is $(\alpha_0 + \alpha_2)^{-1}$ and

the maximum air-gap length is $(\alpha_0 - \alpha_2)^{-1}$.

Substituting equation (3) into (1) and neglecting the higher order harmonics, mutual inductance L_{xy} of the stator windings is given by

$$L_{xy} = K_0[\langle n_x n_y \rangle - \langle n_x \rangle \langle n_y \rangle] - K_2[\langle n_x n_y \cos(2p(¨ - ¯)) \rangle - \langle n_x \rangle \langle n_y \cos(2p(¨ - ¯)) \rangle - \langle n_y \rangle \langle n_x \cos(2p(¨ - ¯)) \rangle] \tag{4}$$

Where coefficients K_0 and K_2 are given by

$K_0 = 2®«_0 rl~_0$ and $K_2 = 2®«_0 rl~_2$

The co-efficients K_0 and K_2 are the machine geometrical constants and can be represented by the machine electrical parameters L_{md} and L_{mq} as expressed in equation (5) & (6) [10]

$$K_0 = \frac{L_{md} + L_{mq}}{2\left[\left(\langle n_x^2 \rangle - \langle n_x \rangle^2\right) - \left(\langle n_x n_y \rangle - \langle n_x \rangle \langle n_y \rangle\right)\right]} \tag{5}$$

$$K_2 = \frac{L_{md} - L_{mq}}{2\left[\frac{1}{2}\sqrt{A_{xx}^2 + B_{xx}^2} + \sqrt{A_{xy}^2 + B_{xy}^2}\right]} \tag{6}$$

Where

$$A_{xy} = \langle n_x n_y \cos(2p¨) \rangle - \langle n_x \rangle \langle n_y \cos(2p¨) \rangle - \langle n_y \rangle \langle n_x \cos(2p¨) \rangle \tag{7}$$

$$B_{xy} = \langle n_x n_y \sin(2p¨) \rangle - \langle n_x \rangle \langle n_y \sin(2p¨) \rangle - \langle n_y \rangle \langle n_x \sin(2p¨) \rangle \tag{8}$$

For, A_{xx} and B_{xx} substitute *y=x* Substituting equation (5) to (8) in (4) is used to calculate the mutual inductances between two arbitrary windings *x* and *y*. To calculate the self inductance *y=x* in (4) can be used. The winding distribution arrangements of *x & y* can be easily found out with the help of the turns function n_x & n_y.

The internal faults in the stator winding do not affect the winding distribution of the rotor windings, however due to change in the winding distribution of the faulted windings of the stator, the mutual inductances between the rotor and the stator should be calculated. The mutual inductance between an arbitrary stator winding *x* and and the damper windings *kd, kq* are given as [10]

$$\left.\begin{matrix} L_{fdx} \\ L_{kdx} \end{matrix}\right\} = L_{md} \frac{\langle n_x \sin(p(¨ - ¯)) \rangle}{\sqrt{\langle n_a \sin(p¨) \rangle^2 + \langle n_a \cos(p¨) \rangle^2}} \tag{9}$$

$$L_{kqx} = L_{mq} \frac{\langle n_x \cos(p(¨ - ¯)) \rangle}{\sqrt{\langle n_a \sin(p¨) \rangle^2 + \langle n_a \cos(p¨) \rangle^2}} \tag{10}$$

The internal fault under a variety of conditions can be simulated with the help of synchronous machine modeling using direct phase quantities as in [13] and the phase currents and individual parallel path currents can be calculated. The rotor windings self and mutual inductances are calculated from the machine standard electrical parameters and its value remain the same even under internal fault conditions. The elements of the inductance matrix of the model based on direct phase quantities are calculated using MWFA under internal fault conditions in the stator windings. The altered values of stator windings self and mutual inductances and stator to rotor mutual inductances under different internal fault conditions can be calculated for salient-pole synchronous generators using (5-10).

3. **Mathematical Model of Synchronous Machines**

The synchronous machines are usually described as a system having 3 stator phases and 3 rotor circuits (one field winding and two damper windings). If the number of parallel paths in the stator is n then the machine can be represented by 3n stator circuits. Under internal fault conditions the number of stator circuits is determined by the number of independent currents flowing in the stator. Therefore, it is convenient to assume *m* stator circuits for the arbitrary stator configuration. Therefore, in terms of flux linkages, ψ, voltage relationships for the stator and rotor circuits, *e*, are linked with the winding resistances *R*, and instantaneous current *I*, as follows,

$$e = \frac{d\cdot}{dt} - Ri \tag{18}$$

Where, $e = [e_1 \;\; e_2 \ldots\ldots\ldots e_m \;\; e_{fd} \;\; e_{1d} \;\; e_{1q}]^t$

$\psi = [\psi_1 \;\; \psi_2 \ldots\ldots\ldots \psi_m \;\; \psi_{fd} \;\; \psi_{1d} \;\; \psi_{1q}]^t$

$R = diag\,[R_1 \;\; R_2 \ldots\ldots\ldots R_m \;\; R_{fd} \;\; R_{1d} \;\; R_{1q}]$

and $i = [i_1 \;\; i_2 \ldots\ldots\ldots i_m \;\; i_{fd} \;\; i_{1d} \;\; i_{1q}]^t$

The flux linkage is expressed as

$$\Psi = L\, i \tag{19}$$

Where, *L* is the inductance matrix given as

$$L = \begin{bmatrix} L_{11} & M_{12} & M_{13} & \cdots & \cdots & \cdots & M_{1m} & M_{1f} & M_{1kd} & M_{1kq} \\ M_{12} & L_{22} & M_{23} & \cdots & \cdots & \cdots & M_{2m} & M_{2f} & M_{2kd} & M_{2kq} \\ M_{13} & M_{23} & L_{33} & \cdots & \cdots & \cdots & M_{3m} & M_{3f} & M_{3kd} & M_{3kq} \\ \vdots & \vdots & \vdots & \cdots & \cdots & \cdots & \vdots & \vdots & \vdots & \vdots \\ \vdots & \vdots & \vdots & \cdots & \cdots & \cdots & \vdots & \vdots & \vdots & \vdots \\ M_{1m} & M_{2m} & M_{3m} & \cdots & \cdots & \cdots & L_{mm} & M_{mf} & M_{mkd} & M_{mkq} \\ M_{1f} & M_{2f} & M_{3f} & \cdots & \cdots & \cdots & M_{mf} & L_{ff} & M_{fD} & M_{fQ} \\ M_{1kd} & M_{2kd} & M_{3kd} & \cdots & \cdots & \cdots & M_{mkd} & M_{fD} & L_{DD} & M_{DQ} \\ M_{1kq} & M_{1kq} & M_{3kq} & \cdots & \cdots & \cdots & M_{mkq} & M_{fQ} & M_{DQ} & L_{QQ} \end{bmatrix} \tag{20}$$

Here, m=3n+1 for fault in any one path

m=3n+2 for fault between two paths

and n= no. of parallel paths.

Therefore, the inductance matrix is of the order of m+3 i.e. the m stator paths and 3 rotor circuits. The inductances calculated using the Modified Winding Function Approach with the help of turn's function of the individual machines is substituted in this inductance matrix for individual cases of internal fault simulation. The rotor's self and mutual inductances are directly calculated using machine parameters and do not change for internal faults in the stator winding.

When the machine is supplying through a short transmission line (fig. 1), the machine terminal voltages can be expressed as

$$e = V - iR_e - i\frac{dL_e}{dt} - iR_g - i\frac{dL_g}{dt} \quad (21)$$

Where, R_e & L_e are both m-by-m diagonal matrices and the elements are the resistance R_e and inductance L_e of the short transmission line respectively,
R_g & L_g are both m-by-m diagonal matrices and the elements are the grounding resistance R_g and inductance L_g respectively, of the generator to limit the fault current.
V represents the m-by-1 infinite bus phase voltage vector.
The equation of motion of a synchronous generator can be expressed by,

$$\frac{d^2¢}{dt^2} = \frac{\mu}{2H}\left(T_{mech} - T_{elec}\right) \quad (22)$$

Where ω is the synchronous speed, H is the inertia constant,
T_{mech} is the mechanical input torque, T_{elec} is the electrical torque.
The electrical torque is given by

$$T_e = \frac{1}{2} i_s^T \frac{\partial L_{ss}}{\partial^-} i_s + i_s^T \frac{\partial L_{rs}}{\partial^-} i_r \quad (23)$$

Where $i_s = [\, i_1 \;\; i_2 \ldots\ldots \; i_m]$ & $i_r = [\, i_f \;\; i_{1d} \;\; i_{1q}]$
L_{ss} is the stator inductance matrix and L_{rs} is the rotor to stator mutual inductance matrix.

The synchronous machine modeling during an internal fault can be done with the help of (18-23). The elements of the inductance matrix can be calculated for salient-pole machines using (4-6, 16-17) and non-salient pole machines (10, 14-17).

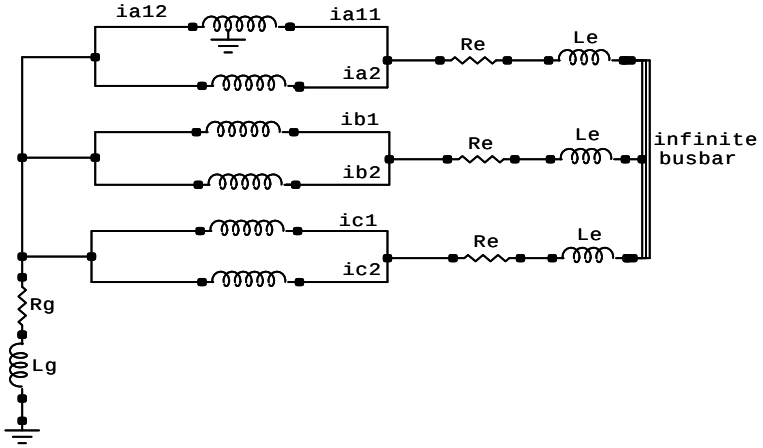

Fig.1 System representation of synchronous generator with two parallel paths during a turn-to-ground fault

4. Fault Simulation Results

A three phase, 76 MVA, 11 KV, 18-pole salient-pole synchronous generator has been considered for modeling, simulation and designing of the intelligent protection scheme. This generator has 216 slots with double layer wave winding arrangement and two parallel paths per phase. Fig 1 shows the circuit representation of the generator under consideration. The winding arrangement of phase a_1 has been shown in fig.2 and its electrical parameters are given in appendix. The turns function of the phase distribution of phase a along the entire periphery of the stator has been shown in fig.3.
The inductances are derived directly from the original waveforms using winding functions of the actual machine winding distribution; hence the space harmonics are taken into account. The machine electrical parameters are used to simplify the calculation of the machine inductances. The investigation of currents in all parallel paths of the phases is an advantage of this model. The machine model has been simulated in the MATLAB/ SIMULINK environment and has been solved using TR-BDF2 solver (an implicit Runga-Kutta formula with a first stage that is a trapezoidal rule step and a second stage that is a

backward differentiation formula of order two). Since the elements of inductance matrix depends on the position of the rotor θ, the matrix L and its inverse have to be evaluated at each step in order to determine the current.

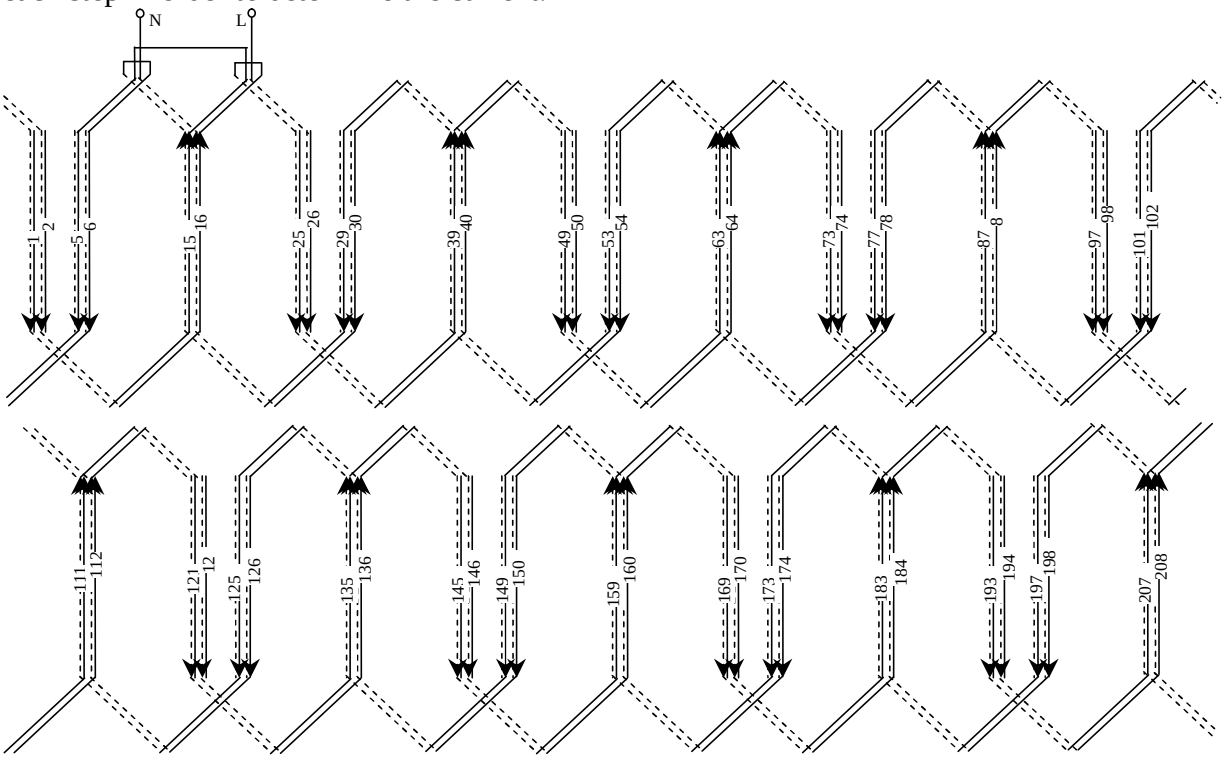

Fig. 2 Wave winding distribution diagram of phase a_1 of the salient-pole synchronous generator

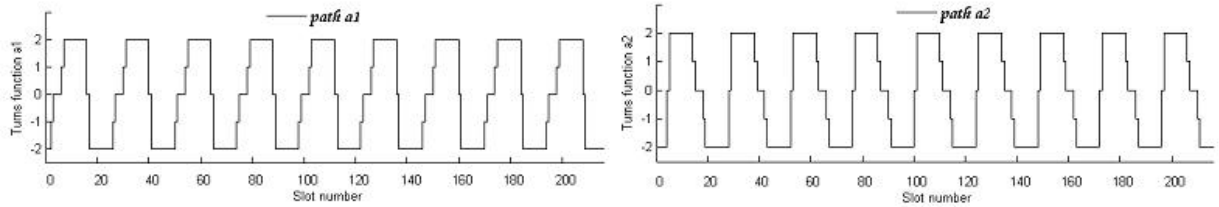

Fig. 3 Turns function of parallel paths of phase *a* of the salient-pole synchronous generator under steady state normal condition.

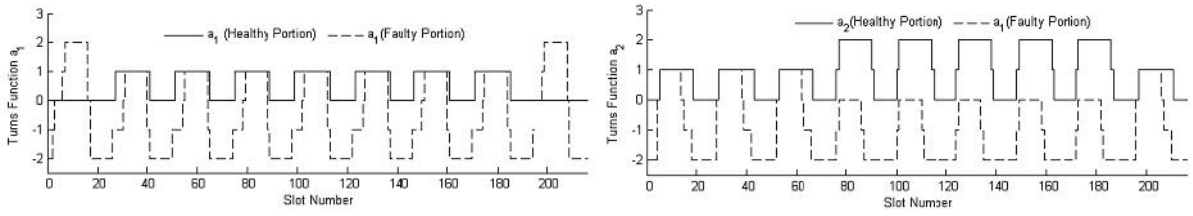

(a)

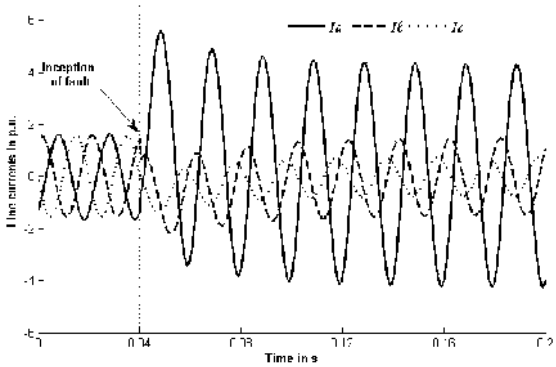

(b)

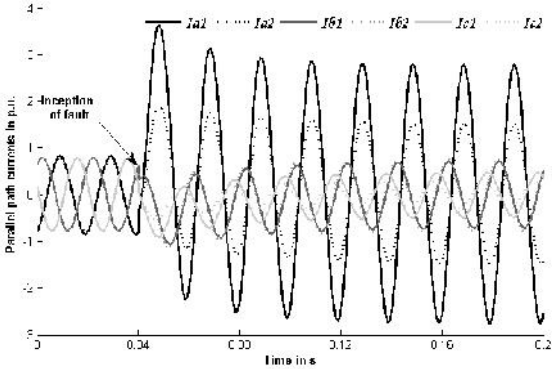

(c)

Fig. 4 Example of internal fault simulation for turn-to-turn fault between path a_1 at 81% and a_2 at 61% from neutral near slot 198 (a) turns function of path a_1 & a_2 (b) the phase currents (c) the parallel path currents.

Fig.4 shows the turns function, phase currents and parallel path currents for turn-to-turn fault at 0.04s between parallel paths of the same phase a near slot number 198 i.e. 81% of path a_1 and 61% of path a_2 is faulty from the neutral. Similarly phase currents and parallel path currents for different cases of turn-to ground fault, turn-to-turn fault between parallel paths of same phase and other phases have been simulated deriving turns function of the individual case. The current of the path in which fault occurs also influences the currents in the healthy portion of the other paths with which it shares the slot in the winding arrangement of the stator. These changes have been considered in the design of the different intelligent protection schemes.

5. Application of MFNN & RBFNN to Generator Protection

In order to detect an internal fault, and differentiate it with steady state normal and external fault conditions, an intelligent protection scheme has been designed using the neural network toolbox of MATLAB. Based on pattern classification, different architectures of both the networks have been trained and tested for only detection of internal fault, detection & classification of internal fault in different phases, and detection & classification of internal fault in parallel paths of the three phases of the stator winding. These protection schemes are based on non-differential pattern classification of currents i.e. the currents have been sampled only at the terminal end of the synchronous generator. One set of data comprises of the samples of currents for one complete cycle sequentially arranged for all the phases or all the parallel paths as required by the problem. A set of 2100 samples comprising of a variety of faults at different locations in the stator winding, with different inception angles including 200 steady state samples has been used for training the neural networks. The training of the networks has been done using a P8300, core2 duo-processor, 2.4GHz.

Different architectures of Multi-Layer Feed-Forward Network have been trained and tested based on pattern classification. 20% of the total number of data sets comprising various cases has been used for testing as well as 20% for validating, and the remaining 60% has been used for training. The feed-forward network has been trained using the gradient descent with momentum back propagation training function and gradient descent with momentum weight/bias learning function. The learning rate has been chosen as 0.1 and the momentum constant as 0.9. The hyperbolic tangent transfer function has been used for all the hidden layers and the output layer. The sigmoidal function helps in producing an arbitrary decision boundary with smooth curves and edges. The training was done for 100,000 iterations. Concerning the ANN architecture, parameters such as the number of hidden layers and the number of neurons in the hidden layers were decided empirically.

In designing a RBFNN, selection of proper values of error goal and spread constant is important. The error goal indicates the closeness of the desired and the actual output. Obviously, a lower value of error goal implies higher accuracy, greater number of neurons in the hidden layer, and more training time. The spread determines the width of the radial basis functions. The spread should be larger than the minimum distance and smaller than the maximum distance between the input vectors. 20% of the total number of samples has been arbitrarily chosen for testing and the remaining 80% has been used for training the radial basis function neural network.

5.1 Internal Fault Detection

48 input neurons and 3 output neurons are required for designing a network for the detection of the fault and differentiate it with the normal and external fault conditions. These 48 input neurons represent the discrete samples of three phase currents in per unit at

a sampling rate of 16 samples per cycle per phase for pattern recognition. The three output neurons represent the normal condition, internal fault and external faults respectively.

The training process of MFNN involves much experimentation with various network configurations. A three layer network with 15 to 96 neurons in the hidden layer has been trained for 100,000 iterations. The performance of various architectures of the networks has been observed and the same has been categorized as not good, good, and best. The training time varied from 92 to 125 minutes.

The RBFNN for fault detection has been trained with different spread constants ranging from 1 to 20 and the error goal being fixed at 0.0001. The number of neurons in the network depends on the training error goal.

5.2 Internal Fault Detection & Classification of Phases

Designing a network for the detection and classification of the fault in phases and differentiating it with the normal and external fault conditions simultaneously requires 48 neurons as input and 5 neurons as output. The three line currents in per unit has been represented by 48 input neurons with a sampling frequency of 800Hz i.e. 16samples/cycle/phase. The five output neurons represent the normal condition, internal faults in the three phases, and external faults respectively.

Various network configuration of three layer network from 15 to 100 neurons in the hidden layer does not give the desired result even after increasing the number of iterations. Therefore after much experimentation two hidden layer feed-forward network architecture with 90 neurons in the first hidden layer has been chosen. Different architectures have been trained with 20 to 80 neurons in the second hidden layer and the performance has been observed. The training time varied from 85 to 125 minutes.

The training and testing of RBFNN has been done with an error goal of 0.0001 and different spread constants from 0.5 to 15. The training error goal and the spread constant for a network being trained give the number of neurons in the protection scheme.

5.3 Internal Fault Detection & Classification of Parallel Paths

The currents sampled at a frequency of 800Hz in two parallel paths of the three phases have been used for detection and classification of internal faults in one or more parallel paths. The 16 samples per cycle per phase per parallel path are represented by 96 input neurons for this protection scheme. The eight output neurons represent the normal condition, internal faults in two parallel paths of each of the three phases, and external faults respectively.

The training of a three layer MFNN with 30 to 192 neurons in the hidden layer for 100,000 epochs does not give the desired result. Therefore the performance of the two hidden layer feed-forward network architecture with 120 neurons in the first hidden layer and 40 to 112 neurons in the second hidden layer has been observed during training. The training time varied from 103 to 144 minutes for different architectures.

The RBFNN has been trained for detection and classification of internal fault any parallel path of the three phases with different spread constants ranging from 1 to 20. The error goal has been fixed at 0.0001. The number of neurons selected for the network depends on the training error goal.

Table 1 and Table 2 show the performance of the various architectures during training for MFNN and RBFNN networks respectively. The performance of the trained network has been designated as not good, good and best. The designation of the network is based on errors observed during training. The network which gives minimum error in combination has been designated as the best and the same has been selected for the final testing of various protection schemes.

The moving data window has been used for the final testing of the selected network for various architectures of both the types of network. The test results for the same have been

tabulated from the instant of fault inception to show the effectiveness of different protection schemes.

Table 1: Neurons in hidden layers and errors during training for different architectures of MFNN

Types of Networks	Network Architecture	Training Error	Testing Error	Validation Error	Performance
MFNN Fault Detection (Neurons in Input Layer = 48, Neurons in Output Layer = 3)	48 *x* 12 *x* 3	0.004	0.0136	0.0114	Not Good
	48 *x* 30 *x* 3	0.0012	0.0033	0.0028	Not Good
	48 *x* 45 *x* 3	0.0009	0.0029	0.0027	Good
	48 *x* 64 *x* 3	0.0008	0.0032	0.0054	Not Good
	48 *x* 72 *x* 3	0.0007	0.0032	0.0023	Good
	48 *x* 84 *x* 3	0.0006	0.0012	0.0013	Best
	48 *x* 96 *x* 3	0.0006	0.0024	0.0030	Good
MFNN Phase Fault Detection & Classification (Neurons in Input Layer = 48, Neurons in Output Layer = 5)	48 *x* 20 *x* 5	0.023	0.036	0.036	Not Good
	48 *x* 42 *x* 5	0.014	0.03	0.029	Not Good
	48 *x* 60 *x* 5	0.012	0.026	0.026	Not Good
	48 *x* 90 *x* 5	0.009	0.019	0.023	Not Good
	48 *x* 120 *x* 5	0.01	0.022	0.024	Not Good
	48 *x* 90 *x* 30 *x* 5	0.0014	0.0114	0.014	Good
	48 *x* 90 *x* 60 *x* 5	0.0007	0.0083	0.0118	Best
	48 *x* 90 *x* 75 *x* 5	0.0012	0.0146	0.0129	Good
MFNN Parallel Path Fault Detection & Classification (Neurons in Input Layer = 96, Neurons in Output Layer = 8)	96 *x* 40 *x* 8	0.0053	0.0126	0.0114	Not Good
	96 *x* 64 *x* 8	0.0034	0.0091	0.0081	Not Good
	96 *x* 96 *x* 8	0.0026	0.0066	0.0061	Not Good
	96 *x* 120 *x* 8	0.0022	0.0037	0.0046	Not Good
	96 *x* 192 *x* 8	0.0020	0.0038	0.0045	Not Good
	96 *x* 120 *x* 60 *x* 8	0.0003	0.0026	0.0024	Good
	96 *x* 120 *x* 72 *x* 8	0.0002	0.0016	0.0020	Best
	96 *x* 120 *x* 96 *x* 8	0.0003	0.0030	0.0029	Good

Table 2: Hidden Neurons and errors for different Spread Constants during training of RBFNN

Types of Networks	Spread Constant	Neurons in Hidden Layer	RMS Errors of Training	RMS Errors of Testing	Performance
RBFNN Fault Detection (Neurons in Input Layer = 48, Neurons in Output Layer = 3)	2	900	0.0276	0.2617	Not Good
	8	925	0.0060	0.2112	Not Good
	13	925	0.0099	0.0425	Best
	16	925	0.0100	0.0535	Good
RBFNN Phase Fault Detection & Classification (Neurons in Input Layer = 48, Neurons in Output Layer = 5)	1	1325	0.0099	0.3270	Not Good
	3	1200	0.0100	0.1301	Good
	4.5	1200	0.0098	0.1061	Best
	6	1200	0.0100	0.1742	Not Good
	10	1175	0.0100	0.2612	Not Good
RBFNN Parallel Path Fault Detection & Classification (Neurons in	2	1100	0.0103	0.1687	Not Good
	6	850	0.0100	0.0402	Good
	9	875	0.0100	0.0410	Not Good

Input Layer = 96, Neurons in Output Layer = 8)	12	900	0.0100	0.0382	Best
	16	925	0.0100	0.0401	Good

The tabulated result for different types of fault is shown in Table 3 & 4 for various architectures of MFNN and RBFNN respectively. The test result output of the selected RBFNN architecture does not give the desired result for the first few samples from the instant of inception of fault but almost after completion of one cycle the result is close to the target. While the chosen MFNN test result output always lies between 0 & 1 and the fault is detected within quarter to three quarters of the cycle from the instant of fault inception depending on the location of the fault. The faults near to terminal are detected earlier as compared to faults near the neutral of synchronous generator.

6. Conclusion

This paper has discussed the application of both MFNN and RBFNN for the non-differential protection of salient-pole synchronous generators against internal faults. The direct phase quantities and modified winding function approach have been used to simulate different types of internal and external faults using electrical parameters of salient-pole synchronous generators being used in practice. The simulated phase and the parallel path currents at the terminal end have been used for the training and testing of different architectures of both the networks. Both the networks have been used as pattern classifiers for identification and classification of internal faults in phases as well as their parallel paths. Various architectures of the networks have been tested and compared as regards training and testing errors. Finally suitable architectures of both the types of neural nets have been selected and tested for a variety of faults using moving data window. The test results indicate that the proposed MFNN and RBFNN are capable of correctly identifying and classifying all types of fault. The comparison of both the types of neural nets reveals that the training of RBFNN is faster than MFNN. Though both the networks identify the fault correctly but MFNN is more reliable, more accurate and faster than RBFNN in detection and classification of the fault. The proposed networks cannot be generalized as the training of the networks is based on simulated fault currents which in turn depend on the winding function requiring the stator winding details of the particular generator.

Appendix

Electrical parameters of the salient-pole synchronous generator :
76 MVA/11 KV/50 Hz/ Poles 18

Armature Resistance = 0.0043p.u.
Armature Leakage Reactance = 0.15p.u.
Direct Axis Synchronous Reactance = 1.03pu
Direct Axis Transient Reactance = 0.26pu.
Direct Axis Sub-Transient Reactance = 0.17pu.
Quadrature Axis Synchronous Reactance = 0.68pu.
Quadrature Axis Transient Reactance = 0.66pu
Quadrature Axis Sub-Transient Reactance = 0.2pu.
Direct Axis Transient OC Time Constant 6.45 s
Direct Axis Sub-Transient OC Time Constant 2.4 s
Quadrature Axis Transient OC Time Constant 0.95 s

References

[1] Dash P. K., Malik O. P., and Hope G. S., Fast Generator Protection Against Internal Asymmetrical Faults, IEEE Trans. Power App. & Sys., Vol. 96, pp. 1498-1508, 1977.
[2] Sidhu T. S., Sunga B., and Sachdeva M. S., A Digital Technique for Stator Winding Protection of Synchronous Generators, Electric Power Systems Research, Vol. 36, pp. 45-55, 1996.

[3] Meghed A. I., and Malik O. P., An artificial neural network based digital differential protection scheme for synchronous generator stator winding protection, IEEE Trans. Power Delivery, Vol. 14, pp. 86-93, 1999.
[4] Darwish H. A., Taalab A. I., and Kawady T. A., Development and implementation of an ANN-based fault diagnosis scheme for generator winding protection, IEEE Trans. Power Delivery, Vol. 16, pp. 208-214, 2001.
[5] Bhalja B., Maheshwari R. P., Nema S., and Verma H. K., Neuro-fuzzy-based Scheme for Stator Winding Protection of Synchronous Generator, Electric Power Comp. & Sys., Vol. 37, pp. 560-576, 2009.
[6] Moravej Z., Vishwakarma D. N., Singh S. P., Application of radial basis function neural network for differential relaying of power transformer, Comp. and Elect. Engg, Vol. 29, pp. 421–434, 2003.
[7] Tripathi M., Maheshwari R.P., and Verma H. K., Radial basis probabilistic neural network for differential protection of power transformer, IET Gener. Transm. Disttrib., Vol. 2, pp. 43-52, 2008.
[8] Samantaray S. R., Dash P. K., and Panda G., Fault Classification and Location using HS-transform and Radial basis function neural network, Electric Power Sys. Research, Vol. 76, pp. 897-905, 2006.
[9] Ravikumar B., Thukaram D., and Khincha H. P., Application of support vector machines for fault diagnosis in power transmission system, IET Gener. Transm. Disttrib., Vol. 2, pp. 119-130, 2008.
[10] Tu X., Dessaint L. A., Fallati N., and Kelper B. D., Modeling and Real-Time Simulation of Internal Faults in Synchronous Generators with Parallel-Connected Windings, IEEE Transactions on Ind. Elect., Vol. 54 pp. 1400-1409, 2007.
[11] Faiz J. and Tabatabaei I., Extension of Winding Function Theory for Uniform Air-Gap in Electric Machinery, IEEE Trans. on Magnetics, Vol. 38, pp. 3654-3657, 2002.
[12] Krause P. C., Wasynczuck O., and Sudhoff S. D., Analysis of Electric Machinery and Drive System, IEEE Press, New York, 1995.
[13] Sinha A., Vishwakarma D. N., and Srivastava R. K., Modeling and Simulation of Internal Faults in Salient-pole Synchronous Generators with Wave Windings, Electric Power Components & Systems, Vol. 38, pp. 100-114, 2010.
[14] Joorabian M., Taleghani M. A., Aggarwal R. K., Accurate fault Locator for EHV transmission lines based on Radial Basis Function Neural Networks, Electric Power Systems Research, Vol. 71, pp. 195-202, 2004.

Table 3: Test Result of MFNN for the selected architecture using moving data window from the instant of inception of fault

	Sample No.	1	2	3	4	5	6	7	8	9	10	11	12	13	14	15	16
Test Result of *48x84x3* network for fault in path c_1 at 42% from neutral.	O_1 Normal	0.935	0.883	0.657	0.312	0.517	0.441	0.195	0.045	0.093	0.096	0.103	0.224	0.448	0.392	0.143	0.016
	O_2 Int.	0.051	0.103	0.305	0.484	0.582	0.871	0.971	0.996	0.996	0.995	0.994	0.962	0.832	0.883	0.966	0.998
	O_3 Ext.	0.007	0.003	0.001	0	0	0	0	0	0	0	0	0	0	0	0	0
Test Result of *48x84x3* network for external line to ground fault.	O_1 Normal	0.857	0.666	0.698	0.822	0.657	0.159	0.026	0.046	0.091	0.058	0.044	0.086	0.135	0.099	0.036	0.019
	O_2 Int.	0.03	0.077	0.047	0.026	0.008	0.008	0.049	0.025	0.026	0.014	0.007	0.005	0.001	0.001	0.003	0.001
	O_3 Ext.	0.029	0.052	0.12	0.236	0.329	0.478	0.407	0.574	0.599	0.615	0.82	0.896	0.942	0.971	0.915	0.988
Test Result of *48x90x60x5* network for fault between path b_1 at 92% & b_2 at 72% from neutral.	O_1 Normal	0.973	0.778	0.444	0.225	0.279	0.118	0.082	0.064	0.035	0.001	0	0	0	0	0	0
	O_2 phase a	0.001	0.002	0	0	0	0	0	0	0	0	0	0	0	0	0	0
	O_3 phase b	0.058	0.994	1	1	1	1	0.995	1	1	1	1	1	1	1	1	1
	O_4 phase c	0.006	0	0	0	0	0.001	0.428	0.923	0.664	0.141	0.04	0.014	0	0.007	0.003	0.006

	O_5 Ext.	0.004	0	0.001	0	0	0	0	0.002	0.002	0	0	0	0	0	0	0
Test Result of *96x120x72x8* network for fault between path a_1 at 75% & a_2 at 56% from neutral.	O_1 Normal	0.978	0.949	0.789	0.422	0.162	0.087	0.086	0.07	0.019	0.002	0.001	0.004	0.001	0.003	0.001	0.001
	O_2 path a_1	0	0	0.001	0.058	0.982	0.999	1	1	1	1	1	1	1	1	1	1
	O_3 path a_2	0.003	0.004	0	0	0	0.015	0.155	0.156	0.552	0.975	0.999	0.993	0.981	0.996	0.995	0.91
	O_4 path b_1	0.001	0.005	0.008	0.004	0	0	0	0	0	0	0	0	0	0	0	0
	O_5 path b_2	0.001	0.001	0.002	0.001	0	0	0	0	0	0	0	0	0	0	0	0
	O_6 path c_1	0.001	0.001	0.003	0.001	0	0	0	0	0	0	0	0	0	0	0	0
	O_7 path c_2	0.001	0.003	0.092	0.951	0.901	0.091	0.027	0.43	0.985	0.987	0.296	0.047	0.016	0.001	0	0.001
	O_8 Ext.	0.006	0.001	0	0	0	0	0.001	0.003	0.003	0.009	0.039	0.104	0.099	0.05	0.027	0.009

Table 4: Test Result of RBFNN for the selected architecture using moving data window from the instant of inception of fault

	Sample No.	1	2	3	4	5	6	7	8	9	10	11	12	13	14	15	16
Test Result of 48x3 network S.C. 13 for fault in path a1 at 75%	O_1 Normal	1.476	3.016	2.587	-0.3	-1.24	-1.294	-3.721	-6.439	-7.575	-7.256	-5.574	-4.042	-2.85	-0.314	0.745	0.018
	O_2 Int.	-0.06	-1.121	-0.87	1.416	2.33	2.609	4.657	6.94	8.154	8.147	6.692	5.067	3.776	1.74	0.68	0.972
	O_3 Ext.	-0.416	-0.895	-0.717	-0.117	-0.09	-0.315	0.064	0.499	0.42	0.109	-0.117	-0.025	0.073	-0.426	-0.425	0.01
Test Result of 48x3 network with S.C. 13 for an external L-G fault	O_1 Normal	0.822	1.356	3.588	3.976	2.544	0.11	-0.912	-0.311	-1.767	-3.89	-4.15	-4.214	-3.763	-2.419	-0.409	0.093
	O_2 Int.	0.829	0.779	-1.051	-1.947	-1.256	1.016	2.211	1.642	2.456	3.451	2.982	3.15	3.398	2.881	1.394	-0.113
	O_3 Ext.	-0.651	-1.135	-1.537	-1.029	-0.288	-0.126	-0.3	-0.331	0.311	1.439	2.167	2.065	1.365	0.538	0.014	1.02
Test Result of 48x5 network with S.C. 4.5 for fault in path b_2 at 50% from neutral.	O_1 Normal	0.729	0.727	1.036	1.015	0.78	0.687	0.465	0.258	0.107	-0.074	-0.24	-0.082	0.022	-0.088	-0.15	0.002
	O_2 phase a	4.827	4.996	1.446	0.312	0.702	0.59	0.477	0.116	0.527	2.03	2.714	2.706	2.752	2.737	2.937	0.019
	O_3 phase b	-1.538	-1.819	-1.439	-0.408	0.391	0.807	1.13	1.294	1.236	1.24	1.271	0.909	0.731	0.677	0.338	0.976
	O_4 phase c	-1.135	-0.963	-0.586	-0.492	-0.213	-0.2	0.137	0.384	0.19	0.015	0.47	0.644	0.213	-0.096	-0.457	-0.017
	O_5 Ext.	0.251	0.198	0.014	-0.02	-0.03	0.054	-0.06	-0.003	0.061	-0.051	-0.066	-0.057	-0.059	-0.015	0.062	0.004
Test Result of 96x8 network with S.C. 12 for fault between path c_1 at 75%) & c_2 at 56% from neutral.	O_1 Normal	2.66	2.765	2.123	3.949	7.022	8.416	7.528	4.273	1.162	-1.233	-3.884	-2.217	2.175	3.229	1.634	-0.003
	O_2 path a_1	-2.01	0.545	2.138	0.494	-0.779	-0.335	1.239	1.03	-1.615	-2.206	0.148	1.17	0.791	-0.888	-0.23	-0.018
	O_3 path a_2	-0.719	-2.799	-5.315	-6.758	-5.417	-3.414	-2.573	0.132	3.523	4.978	4.419	0.22	-5.024	-3.092	0.83	-0.026
	O_4 path b_1	0.357	0.727	1.583	1.591	0.755	0.772	0.148	-1.839	-2.224	-1.034	-1.538	-2.574	-0.778	-0.753	-2.337	0.001
	O_5 path b_2	0.513	-1.856	-2.107	-0.796	-0.441	-0.282	-0.493	-0.419	1.122	2.301	1.249	-1.415	-2.09	-3.021	-3.46	0.014
	O_6 path c_1	-1.651	-0.71	2.669	4.097	2.874	0.363	-1.458	-1.265	0.786	4.074	5.154	1.9	-1.977	-4.974	-2.905	1.016
	O_7 path c_2	-3.814	-3.816	-2.191	-0.786	-0.841	-1.878	-2.749	-3.72	-2.66	1.168	3.594	1.976	0.135	-3.606	-4.03	0.999
	O_8 Ext.	-0.669	-0.508	-0.277	-1.555	-3.21	-3.741	-3.203	-1.571	-0.189	0.696	2.047	1.574	-0.328	-0.318	0.303	0.003